Biointerface Research in Applied Chemistry
Open-Access Journal (ISSN: 2069-5837)

Article
Volume 13, Issue 3, 2023, 295
https://doi.org/10.33263/BRIAC133.295

In Sight on the Enhancement of Optical and Structural Properties of Polyamide-6 Fibers

Mohammed A. El-Bakary [1,*], Issam H. Al-Ahdali [2]

[1] Physics Department, Faculty of Science, Mansoura University, Mansoura, Egypt; elbakary2@yahoo.com (M.A.El-Bakary);
[2] Physics Department, Faculty of Science, King Abdulaziz University, Jeddah, Saudia Arabia; ialahdli@yahoo.com (I.H.Al-Ahdali);
* Correspondence: elbakary2@yahoo.com (M.A.El-Bakary);

Scopus Author ID 6603639038

Received: 27.12.2021; Accepted: 24.01.2022; Published: 12.07.2022

Abstract: The work aims to modify the physical properties and structural parameters of Polyamide-6 fiber to be available for different applications through the annealing process. Polyamide-6 samples were annealed at every 10 degrees of temperatures ranging from 60 to 130 ±1°C when the time is constant (2 hours). The computer-aided two-beam polarizing interference microscope attached with variable wavelength interference filter (VAWI- technique) was used to achieve the optical measurements. The device was installed and calibrated using a software program to obtain a sharp two-beam interference pattern and sharp fringes inside the fiber. A CCD camera was used to transfer the microinterferograms to the image analysis screen to automatically measure the index of refraction and optical anisotropy of polyamide-6 fibers before and after the annealing process. To detect the improvements of the fiber structure, the oscillation and dispersion energies, dielectric constant, orientation factor, density, and crystallinity degree were calculated. The results shed light on the structural improvements of Polyamide-6 fibers on the molecular level.

Keywords: VAWI technique; Polyamide-6 fibers; annealing; birefringence; orientation factor.

1. Introduction

Years ago, synthetic polymer fibers such as polyamides had been the backbone of many industrial applications. They are widely used in textile, reinforcement of car tires, automotive, aerospace, transportation markets, microelectronics, airbags, wind energy, and medical devices such as sutures [1-3]. Polyamide-6 is one of the polyamide's family and has remarkable physical properties that enable it to be used in limited applications [4, 5]. For successful use in different applications, it is necessary to obtain oriented fiber structures to realize sufficiently high tenacity and strength, stiffness to weight ratio, and remove the large irreversible deformation inherent in un-oriented flexible polymers [6-8]. One of the most available techniques for developing polymer fibers' molecular orientation and structural properties is the annealing process [9,10]. The choice of the annealing temperature between the glass transition and melting points is important in improving the crystallinity in the semi-crystalline polymer. Annealing near the melting temperature leads to partial melting and increases in mobility. Many authors [11-13] have studied the impact of the annealing process on the structure development of synthetic polymer fibers.

The principle optical properties are recognized in polymer fibers as the main structural information source describing the functional behavior related to the fiber end-use. The refraction index measures the velocity of light inside the medium and is related to the polarizability of the chains. It is related to important structural parameters such as; the dielectric constant and polarizability per unit volume [14]. Birefringence is a good indicator for average orientation in polymer material. It is the average of the crystalline and amorphous regions [15]. Birefringence is the material optical property of having a refractive index that depends on the light polarization direction. During manufacturing, polymers suffer a lot of stress that could cause the undesirable orientation of the molecular chains. These oriented chains split the incident electromagnetic wave into two waves with different optical paths, which causes double refraction [16]. Birefringence spectroscopy is based on this phenomenon as it can be used to investigate the molecular orientation in polymer materials by determining the retardation of the polarized light transmitting through the sample. The sum of the polarizability of all molecular chains in the polymer sample gives rise to the total birefringence. The relationship between molecular orientation and birefringence makes this experimental technique promising [17].

Interference microscopy is a valuable tool for characterizing fibers' properties [18-21]. They are suitable methods for measuring the local index of refraction and birefringence, which are generally good indicators of the orientation of the molecules and hence the fluctuations in density [22, 23]. The VAWI- technique is an interferometric technique developed to automatically detect the refraction effects at any wavelength in the visible spectrum. Many authors have cited the analysis and application of this technique [19]. The advantage of this technique other than traditional interferometric techniques is that it is sufficient to measure the number of interfering spacings produced in the interference pattern of the object under test. So that it does not require immersion media, it works in air media. Using this technique, the optical properties and the refractive index profile of highly oriented fibers were determined [24, 25], and the radial structural parameters of PEEK fibers were investigated [26].

Material dispersion is a very important parameter by which the wavelength-dependent interaction with the material spreads out the incident electromagnetic wave. The degree of the dispersion is a function of the source spectral width, the range of optical frequencies propagating in the medium, and the atomic structure. The atomic structure assumes a dipole moment as it experiences the electromagnetic field induced by the propagating light, which results from a change in the velocity of light [27].

In this work, a computer-aided VAWI interferometric technique was installed and calibrated to investigate the dispersion properties of annealed polyamide-6 fibers. The effects of the incident's interaction with variable wavelength are investigated by verifying Cauchy's and Sellmeier's equations and determining their constants. Some structural relationship properties of polyamide-6 fibers are determined to confirm the development in the structural parameters due to the annealing process. The opto-thermal properties of different samples of polyamide-6 fibers were investigated.

1.1.Theoretical background of the VAWI Technique.

The VAWI method's principle depends on using the two-beam polarizing interference microscope equipped with a continuously variable interference filter. The two-beam interference pattern has an intensity **I** may approximately be expressed as follows [19]:

$$\mathbf{I = I_{max} \sin^2(\varphi / 2) = I_{max} \sin^2(\pi \delta / \lambda)} \quad (1)$$

Where φ is the the phase and δ is the optical path difference in either direction of the polarized light vector (∥ and ⊥) where ($\delta = \varphi\lambda/2\pi$). From the interference patterns, the refractive index n of the fiber under test can be determined at a different wavelength λ of used light. This makes it possible to determine the dispersion of the refractive index n(λ).

Select a certain wavelength λ_1 from the higher wavelength regions for which the center of the interference pattern is maximally dark (coincidence position). This situation can be described as:

$$\delta_1^{\parallel} = (n_1^{\parallel} - 1)t = (m_1^{\parallel} + q_1)\lambda_1, \qquad (2)$$

Where $m_1^{\parallel}$ is the initial interference order that takes an integer value, $n^{\parallel}$ is the refractive index of the fiber in this direction. Decreasing the wavelength to another certain wavelength λ_2 ($\lambda_2 < \lambda_1$) for which the center of the interference pattern becomes maximally bright (anti-coincidence position). By selecting another position of coincidence by transverse sliding, the wedge interference filter. These situations can be described as [19]:

$$\delta_s^{\parallel} = (n_s^{\parallel} - 1)t = (m_1^{\parallel} + q_s)\lambda_s = m_s^{\parallel}\lambda_s,$$
$$\delta_s^{\perp} = (n_s^{\perp} - 1)t = (m_1^{\perp} + q_s)\lambda_s^{\perp} = m_s^{\perp}\lambda_s$$
$$\Delta\delta_s = \Delta nt = (m_1 + q_s)\lambda_s = m_s\lambda_s \qquad (3)$$

The symbols s takes the values from 2, 3, 4, 5,....., and q_s equals 0.5, 1, 1.5, 2, 2.5, 3,….. It expresses the increase in the current interference order, $m_s=(m_1+q_s)$, and then the initial interference order can be given by:

$$m_1 = q_s \frac{b_s}{b_1 - b_s} \qquad (4)$$

b_s refers to the inter-fringe spacing at λs and b_1 corresponding to λ_1. s refers to the coincidence number. So, the VAWI method is an easy and quick method for measuring the spectral dispersion curves of the refractive indices $n^{\parallel}$, $n^{\perp}$, and birefringence Δn of fibers.

2. Materials and Methods

2.1.Sample preparation (annealing).

The annealing temperature strongly affects the structural properties of semi-crystalline polymers, particularly near the transition temperature. The properties change depending on the proportions of amorphous and crystalline phases. The glass transition temperature of Polyamide-6 fiber is T_g =47°C, and the melting point is T_m =215 °C [28]. The Polyamide-6 samples were distributed in eight small glass tubes; then, the tubes were placed in the house of an electric oven at a certain constant temperature within ±l°C. The annealing temperature was selected to be above T_g and blew T_m, so the samples were heated at temperatures ranging from 60 to 130°C within 2h. The samples, after heating, were left to cool at room temperature 25°C.

3. Results and Discussion

The VAWI interferometric technique was installed and calibrated [29]. For the measurement of the fiber thickness, a sample of virgin Polyamide-6 fiber is transferred to the microscope stage after fixing it on a glass slide. Then the microscope is adjusted in a subtractive position. The software program menu was adjusted from the measurement screen to measure

the fiber thickness. The virgin Polyamide-6 sample thickness was measured and was found to be 16.36 ±0.l μm.

The microscope is reconstructed in the position for obtaining a duplicated image of polyamide-6 fiber for measuring the refractive indices. The first refractive index $n^{\parallel}$ of the virgin polyamide-6 sample was measured when the light vector vibrated parallel to the fiber axis. The results are given in Table 1. The spectral dispersion curve can be drawn. Figure 1a gives the microinterferogram of duplicated images for the virgin polyamide-6 fiber sample. The upper image is for the parallel direction of the light vector for measuring the refractive index $n^{\parallel}$, which is the first refractive index. The results were stored in the computer storage media. Then, the program options were adjusted to measure the second refractive index, $n^{\perp}$, with the same process. The refractive index $n^{\perp}$ of the virgin polyamide-6 sample was measured using the VAWI technique, and the results are given in Table 2. Figure 1b shows the printed microinterferograms of duplicated images for the virgin polyamide-6 fiber sample. The lower shift inside the fiber is for the second refractive indx, $n^{\perp}$, in the perpendicular direction of the light vector. The refractive index n measurement has an accuracy of about 0.1%, and it is 0.5nm for the wavelength measurement λ using this technique. It is obvious from Tables 1 and 2 that the interference order is higher in the case of the parallel direction than that of the perpendicular direction and varies with the wavelength variation. This confirms the anisotropic and dispersion properties of the virgin polyamide-6 fiber.

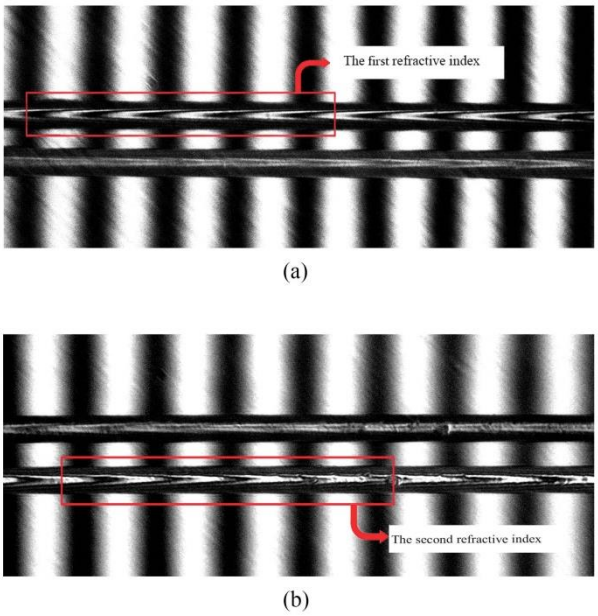

Figure 1. Microinterferograms of duplicated images for polyamide-6 fiber. **(a)** The upper shift for the parallel direction of the light vector, **(b)** The lower shift for the perpendicular direction.

Table 1. Results of the parallel refractive index measurements of the virgin polyamide-6 sample with a thickness of 16.36 μm using the VAWI technique.

s	q_s	b_s (μm)	λ_s (nm)	m_s	$\delta_s^{\parallel}$ (μm)	$n^{\parallel}$
1	0	234.3344	711.1769	13	9.2453	1.565
2	0.5	227.5993	686.4815	13.5	9.2675	1.566
3	1	220.9293	662.4214	14	9.2739	1.567
4	1.5	214.8863	640.9862	14.5	9.2943	1.568
5	2	209.1485	620.9333	15	9.3140	1.569
6	2.5	203.6135	601.8516	15.5	9.3287	1.570
7	3	198.4354	584.2438	16	9.3479	1.571
8	3.5	193.6108	568.0606	16.5	9.3730	1.573
9	4	188.8623	552.2882	17	9.3889	1.574
10	4.5	184.4411	537.7886	17.5	9.4113	1.575

s	q_s	b_s (μm)	λ_s (nm)	m_s	$\delta_s^{\parallel}$ (μm)	$n^{\parallel}$
11	5	180.1413	523.8167	18	9.4287	1.576
12	5.5	176.0352	510.6108	18.5	9.4463	1.577
13	6	172.2153	498.4737	19	9.4710	1.579
14	6.5	168.4777	486.6769	19.5	9.4902	1.580
15	7	164.9783	475.7550	20	9.5151	1.582
16	7.5	161.5243	465.0390	20.5	9.5333	1.583
17	8	158.1642	454.6810	21	9.5483	1.584
18	8.5	155.0100	445.0512	21.5	9.5686	1.585
19	9	152.0687	435.7136	22	9.5857	1.587
20	9.5	149.0706	426.2667	22.5	9.5910	1.587

To measure the birefringence of virgin Polyamide-6 fiber, the microscope is set in the subtractive configuration that the non-duplicated image of the fiber is observed on the monitor parallel to the horizontal direction. The program options were adjusted to measure the dispersion of the birefringence Δn, using the VAWI technique, and the results are given in Table 3. Figure 2 gives microinterferogram of a non-duplicated image for the direct birefringence of virgin polyamide-6 fiber samples.

Table 2. Results of the perpendicular refractive index measurements of the virgin polyamide-6 sample 16.36 μm thick using the VAWI technique.

s	q_s	b_s (μm)	λ_s (nm)	m_s	$\delta_s^{\perp}$ (μm)	$n^{\perp}$
1	0	230.7863	697.3083	12	8.3677	1.511
2	0.5	223.6240	671.5360	12.5	8.3942	1.513
3	1	216.4730	646.2154	13	8.4008	1.514
4	1.5	210.1029	624.0667	13.5	8.4249	1.515
5	2	204.1213	603.5786	14	8.4501	1.517
6	2.5	198.2775	583.8207	14.5	8.4654	1.518
7	3	193.0625	566.4733	15	8.4971	1.519
8	3.5	187.6779	548.7032	15.5	8.5049	1.520
9	4	183.0388	533.6625	16	8.5386	1.522
10	4.5	178.2454	518.2121	16.5	8.5505	1.523
11	5	173.9302	504.5000	17	8.5765	1.524
12	5.5	169.6318	490.9371	17.5	8.5914	1.525
13	6	165.7421	478.8278	18	8.6189	1.527
14	6.5	161.7441	466.4162	18.5	8.6287	1.527
15	7	158.1645	455.4632	19	8.6538	1.529
16	7.5	154.5691	444.4974	19.5	8.6677	1.530
17	8	151.2254	434.41	20	8.6882	1.531
18	8.5	147.9970	424.7366	20.5	8.7071	1.532
19	9	144.7780	415.1190	21	8.7175	1.533
20	9.5	142.0047	406.9907	21.5	8.7503	1.535

The same processes for measuring the thickness, refractive indices, and birefringence were repeated for each sample of the annealed polyamide-6 fiber samples at different temperatures from 60 to 130°C.

Table 3. Results of the birefringence measurements of the virgin polyamide-6 sample 16.36 μm thick using the VAWI technique.

s	q_s	b_s (μm)	λ_s (nm)	m_s	δ_s (μm)	Δn
1	0	187.6462	600.8829	1.5	0.9012	0.0551
2	0.5	211.5022	452.2543	2	0.9045	0.0553

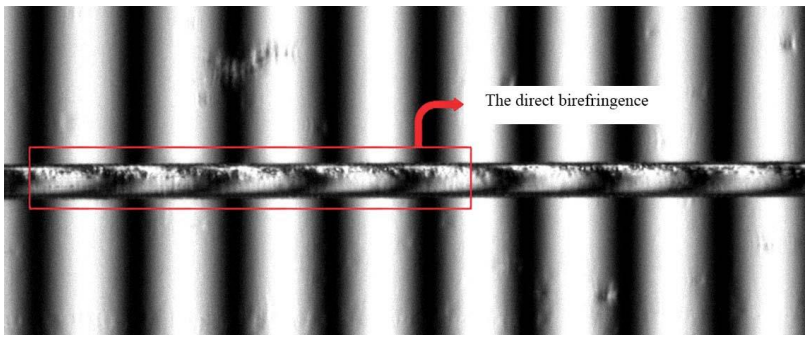

Figure 2. Microinterferogram of non-duplicated image for the direct birefringence of polyamide-6 fiber.

Table 4 gives the results of the thickness measurements of the annealed samples with an accuracy of ±0.l μm. The thickness of the fiber was slightly increased due to the annealing process at different temperatures. The higher the annealing temperature, the higher the sample thickness. Figures 3a and 3b showed the spectral dispersion curves of annealed polyamide-6 samples when the light vector polarized parallel (a) and perpendicular (b) to the fiber axis at different annealing temperatures. The values of the refractive index increased with increasing the annealing temperature in the case of parallel direction, while it decreased in the perpendicular direction. The spectral dispersion curves of the birefringence are given in figure (4). All the annealed polyamide-6 samples have a normal dispersion behavior.

3.1.The impact of the annealing process on the dispersion and structural parameters of polyamide-6 fiber.

The material dispersion behavior was characterized by the temperature dependence of Cauchy's dispersion formula of the form [30]:

$$n(\lambda, T) = A(T) + \frac{B(T)}{\lambda^2} \qquad (5)$$

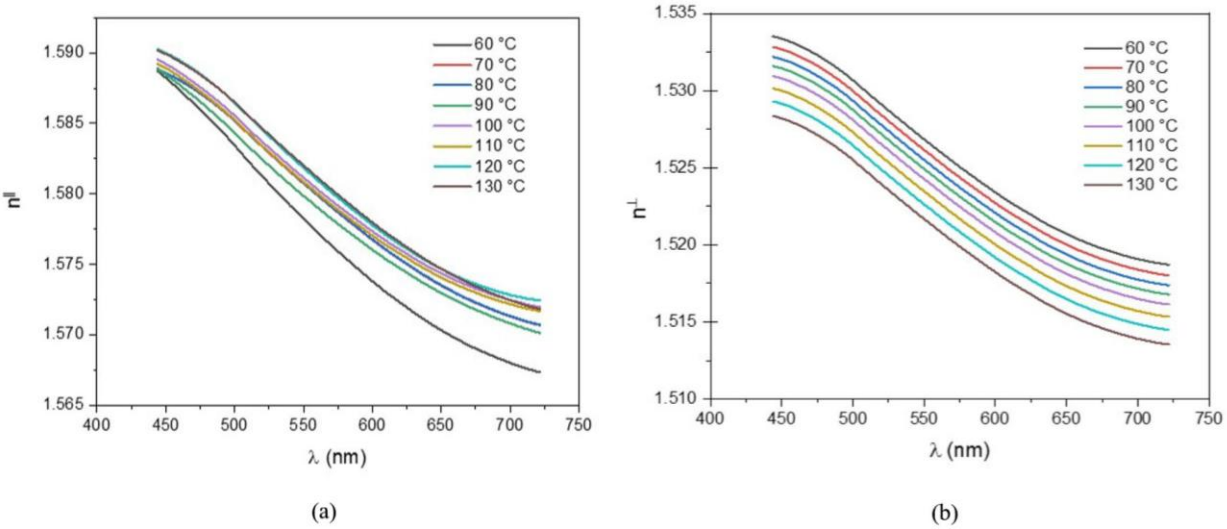

Figure 3. The dispersion of the refractive index of annealed polyamide-6 fibers samples; **(a)** The incident light polarized parallel, $n^{\parallel}$, to the fiber axis, and **(b)** perpendicular, $n^{\perp}$, to the fiber axis.

Table 4. The thickness of virgin and annealed polyamide-6 fiber samples.

Annealing temp. ±l°C	Thickness ±0.l μm
(virgin) Room temp. °C	16.36
60 °C	16.66
70 °C	17.98
80 °C	18.26

Annealing temp. ±l°C	Thickness ±0.l μm
90 °C	18.79
100 °C	18.56
110 °C	19.10
120 °C	19.10
130 °C	20.61

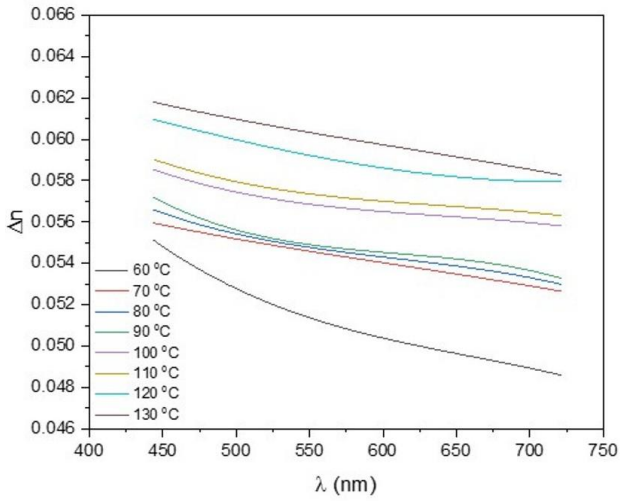

Figure 4. The dispersion of the birefringence of annealed polyamide-6 fiber samples.

Where n(λ, T) is the refractive index at a certain wavelength λ and annealing temperature T. This equation throw light on the material refraction effects with the wavelengths entire the visible spectrum through determining the constants A(T) and B(T). By plotting the relations between the refractive indices $n^{\parallel}$, $n^{\perp}$ and $1/\lambda^2$ for different annealing temperatures as shown in figure 5(a, b), the constants A(T) and B(T) were determined in the two directions of the polarized light. Table 5 gives the values of the constants A and B at different annealing temperatures. The resonance wavelength of the fiber material λ_n is calculated [14,34]. The variation in Cauchy's constants and the natural wavelength with the annealing temperature lighten the internal structure of polyamide-6 fibers. The structural properties in the parallel direction are higher than in the perpendicular direction.

Table 5. The Cauchy's constants of polyamide-6 fibers at the annealing temperatures.

Annealing Temp. °C	Parallel direction			Perpendicular direction		
	$A^{\parallel}$	$B^{\parallel}$ x 10^3 nm^2	$\lambda_o^{\parallel}$ nm	$A^{\perp}$	$B^{\perp}$ x$10^3$$nm^2$	$\lambda_o^{\perp}$ nm
60	1.553	7.404	127.6187	1.50831	5.41003	113.1371
70	1.559	6.446	118.5702	1.50762	5.41003	113.2037
80	1.558	6.449	118.6318	1.50698	5.41003	113.2655
90	1.558	6.453	118.6933	1.50639	5.41003	113.3226
100	1.560	6.209	116.2456	1.50573	5.41003	113.3866
110	1.563	6.209	116.2724	1.50493	5.41003	113.4644
120	1.560	6.442	118.4220	1.50409	5.41003	113.5462
130	1.559	6.519	119.1508	1.50314	5.41003	113.6390

To fully characterize the interaction of incident photon energy E with the fiber materials, some of this energy makes resonance with the electronic oscillation, and the other is dispersed. The dispersion energy is a measure of the strength of inter-band optical transition and is related to chemical bonding. The refractive index frequency dependence, including oscillation and dispersion energies (E_o, E_d) of the bounded electrons of the polyamide-6 fiber material, is given by Sellmeier's equation in the following form [32]:

$$(n^2 - 1)^{-1} = \frac{E_o}{E_d} + \frac{E^2}{E_d E_o} \qquad (6)$$

The linear relationship between $(n^2-1)^{-1}$ and E^2 has a slope of $(1/ E_oE_d)$, and its intercept on the y-axis is the ratio (E_o/E_d). Figure 6(a, b) shows the linear relationships in the two directions of the polarized light. The values of oscillation and dispersion energies E_o, E_d describe the potential interaction behavior of the optical effects in polyamide-6 fiber due to its chemical bond [30].

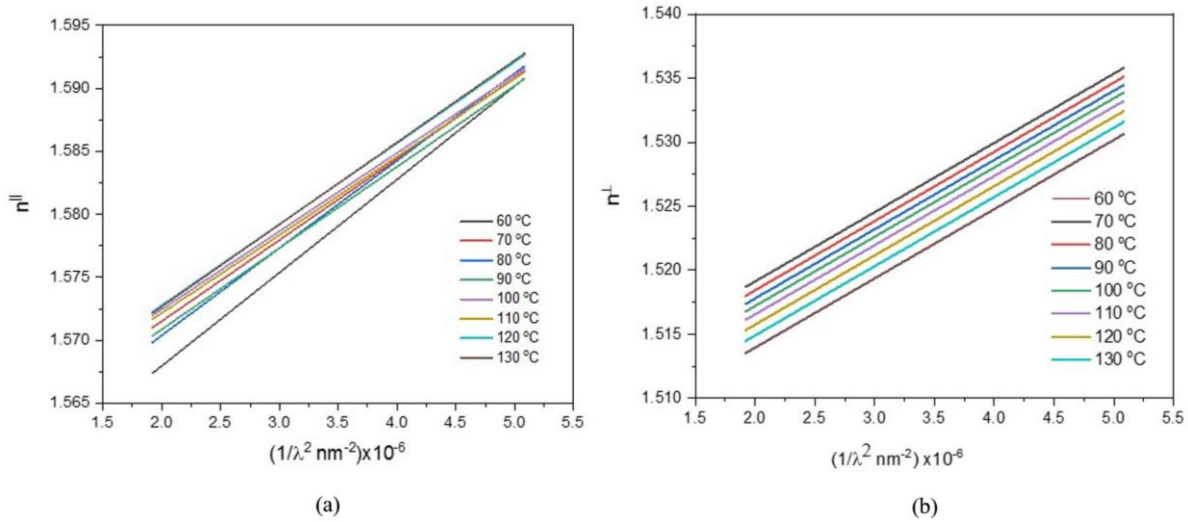

Figure 5. The refractive indices $n^{\parallel}$ (a), $n^{\perp}$ (b) verses $1/\lambda^2$ at different annealing temperatures for polyamide-6 fiber, respectively.

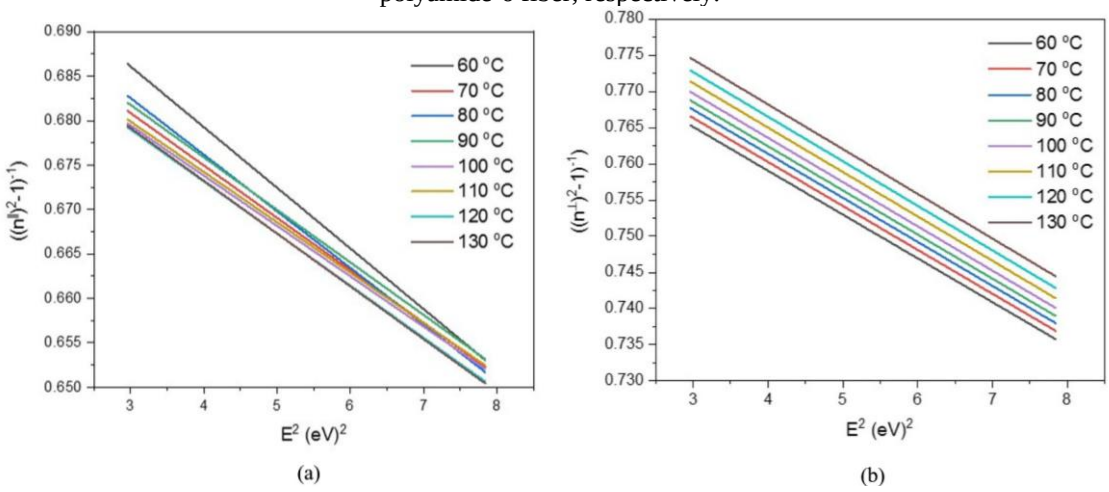

Figure 6. The linear relation between $(n^2-1)^{-1}$ and E^2 at different annealing temperatures for polyamide-6 fiber when the polarized is parallel **(a)** and perpendicular **(b)** to the fiber axis.

Figures 7 and 8 clarify the variation of the oscillation and dispersion energies E_o, E_d, respectively, with the annealing temperature. In the case of polarized light parallel to the fiber axis, the dispersion and oscillation energies increase with the annealing temperature until nearly 100 ^oC, then slowly decrease. Otherwise, the dispersion and oscillation energies decrease linearly in the perpendicular direction. It is recommended that the best annealing temperature is 100 ^oC, which modifies the polyamide-6 fiber.

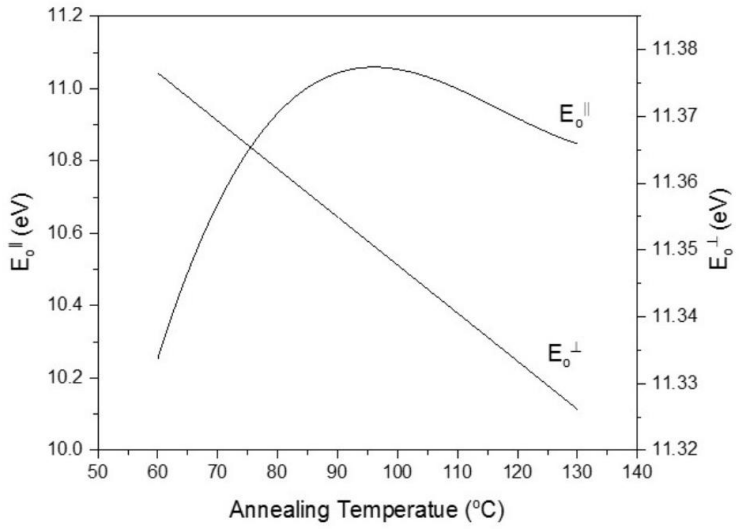

Figure 7. The variation of the oscillation energy with the annealing temperature in both directions of the polarized light.

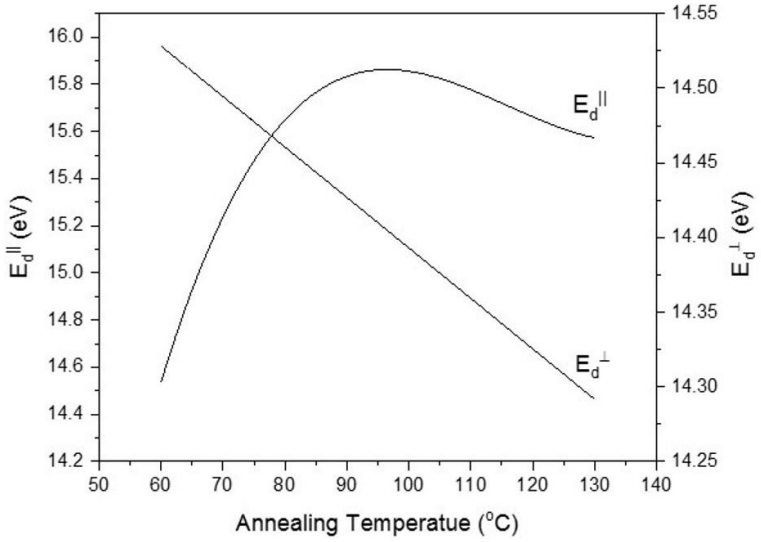

Figure 8. The variation of the dispersion energy with the annealing temperature in both directions of the polarized light.

To characterize the impact of thermal annealing on the structural properties of polyamide-6 fiber, the dielectric constant is an important structural parameter that describes the relative permittivity of the fiber material to the external electric field [27]. It is related to the refractive index of fiber material by the following relation [33]:

$$\varepsilon = \frac{1 + 2(n^2 - 1)/(n^2 + 2)}{1 - 2(n^2 - 1)/(n^2 + 2)} \qquad (7)$$

Figures 9a and 9b give the dielectric constant values at different annealing temperatures for different wavelengths in both directions of the polarized light vibrations. The interpretation of the constant dielectric changes with the annealing temperature sheds light on the variations of the electrical properties resulting in the polyamide-6 fiber samples after annealing. Also, the refractive index is related to the density of the material. It is calculated from the measured refractive indices for the different samples of polyamide-6 fiber at different annealing temperatures by the following equation [35]:

$$\rho = \rho_a \left(\frac{\bar{n}^2 - 1}{\bar{n}^2 + 2} \right) \left(\frac{n_{iso}^2 + 2}{n_{iso}^2 - 1} \right) \qquad (8)$$

where ρ_a is the density of the amorphous regions of polyamide-6 fiber (ρ_a=1110 kg/m^3) [36], $\bar{n}$ is the mean refractive ($\bar{n}=(n^{\parallel}+n^{\perp})/2$), and n_{iso} is the isotropic refractive index ($n_{iso}=(n^{\parallel}+2n^{\perp})/3$). Figure 10 shows that the density increased as the annealing temperature increased at a constant wavelength. The density variation due to annealing temperature results from the reorientation of the molecules that constitutes the polyamide-6 fiber. At different wavelengths, the density variation gives evidence of the inter-chain interaction in polyamide-6 fiber. The reorientation of these molecules can be measured by measuring the birefringence and relating the measured values to the maximum birefringence Δn_{max}. This defines the optical orientation factor $F(\theta)$, as given in the following equation [33]:

$$F(\theta)=\frac{\Delta n}{\Delta n_{max}} \qquad (9)$$

The optical orientation factor was calculated at different annealing temperatures and at certain selected wavelengths using the maximum birefringence for polyamide-6 as Δn_{max}, =0.072 [37]. Figure 11 shows the behavior of the optical orientation factor with increasing the annealing temperature at different wavelengths. The optical orientation factor decreased at high wavelengths.

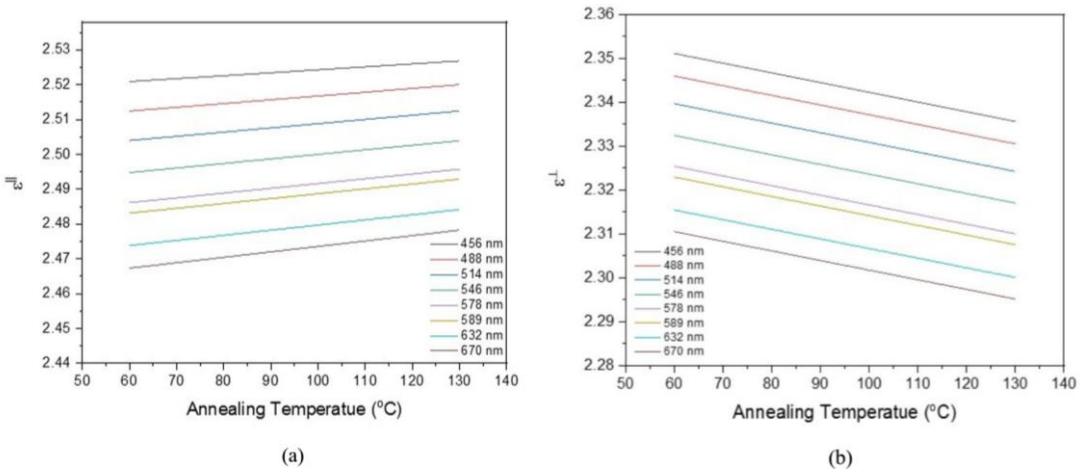

Figure 9. The dielectric constant versus the annealing temperature at different wavelengths. **(a)** parallel direction, **(b)** perpendicular direction.

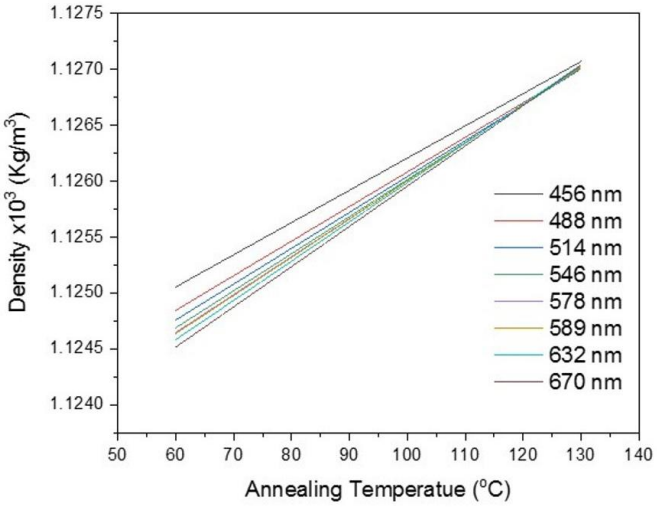

Figure 10. The average density variation with the annealing temperature at different wavelengths.

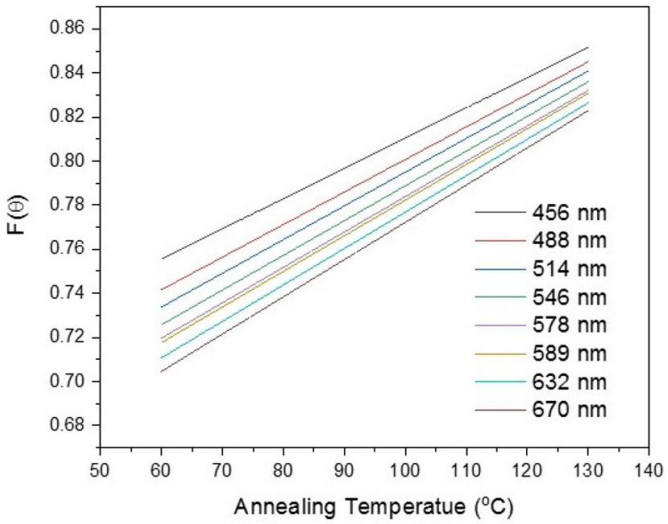

Figure 11. The optical orientation factor versus the annealing temperature at certain wavelengths.

Due to the annealing process, the molecules' orientation in polyamide-6 media leads to some regions being more oriented than others. So that polyamide-6 fibers contain new crystalline regions and new amorphous regions due to each annealing temperature. The density variations of these regions at different annealing temperatures lead to variations in the crystalline regions. The mass fraction of the crystalline regions percentage, χ_m, was calculated depending on the density values by the following relation [35,38]:

$$\chi_m = \frac{\rho_c(\rho - \rho_a)}{\rho(\rho_c - \rho_a)} \qquad (10)$$

where ρ_c and ρ_a are the crystalline regions' density and the amorphous regions' density. ρ_c=1.230 g/cm^3 for polyamide-6 fibers [38]. As polyamide-6 material is a semi-crystalline material that contains different ratios from the crystalline and amorphous regions, the mass fraction of amorphous (1-χ_m) was calculated by;

$$1 - \chi_m = 1 - \frac{\rho_c(\rho - \rho_a)}{\rho(\rho_c - \rho_a)} \qquad (11)$$

Figures 12a and 12b present the relation between the crystalline regions fraction of the crystalline χ_m% (a), amorphous regions (1-χ_m)% (b) percentages versus the annealing temperatures at selected wavelengths. The percentage of crystalline regions χ_m % increased with increasing the annealing temperature and decreased with increasing the wavelength. Otherwise, the mass fraction percentage of amorphous regions (1-χ_m)% is decreased with increasing the temperature and increased with increasing the wavelength. The variation in the crystalline and amorphous regions leads to variations in the refractive indices and birefringence, which mainly depend on the wavelength of light. So, the variation of the mass fraction of the crystalline and amorphous regions with the wavelength are qualitative properties as these parameters are intrinsic structural properties of the material.

The annealing of polyamide-6 fiber varies the dielectric constant, the average density, the degree of orientation, and hence the degree of crystallinity and the other related physical parameters. Studying the structural parameters of modified polyamide-6 samples by annealing is important to establish a connection between these properties and suitable industrial applications. The advantage of using the VAWI technique for these measurements is that they give optical and structural information at any value of the wavelength in the visible spectrum.

4. Conclusions

The annealing temperature affected the optical and structural parameters of polyamide-6 fibers. Increasing the annealing temperature increases the reorientation of the material molecules, which leads to an increase in the optical anisotropy, density optical orientation factor, and mass

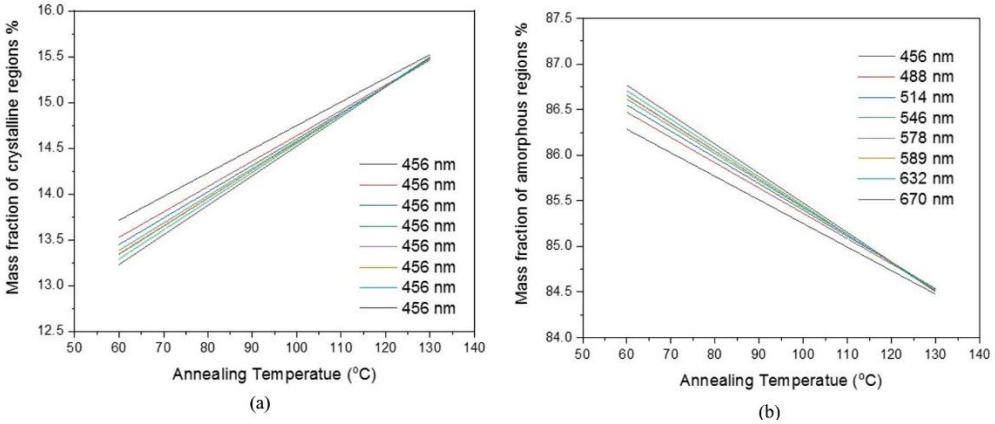

Figure 12. The mass fraction of the crystalline regions χ_m**%(a)** and amorphous regions (1-χ_m%) versus annealing temperatures at different wavelengths.

Fraction of the crystalline regions in fiber materials. So, the annealing process is one of the important methods for modifying the structural and optical properties of polyamide-6.

The computer-aided VAWI technique is an accurate, quick technique suitable for measuring the principal optical properties and thickness of polymer fibers. It enables the determination of the dispersion properties of the index of and birefringence, verifying Cauchy's equation and determining the Cauchy's constants which lighten the arrangement of polyamide-6 fiber molecules. The VAWI technique enables us to determine oscillation and dispersion energy. These results indicate the amount of molecules' orientation along the fiber axis and, therefore, the modification polyamide-6 fiber structure.

Funding

This research was funded by KING AbdULAZIZ for Science and Technology (KACST), KSA, under research project AT-27-5.

Acknowledgments

The authors would like to express their profound thanks to Prof. A.A. Hamza, Professor of Physics and Ex-president of Mansoura University and British University in Egypt, for his valuable discussions.

Conflicts of Interest

The authors declare no conflict of interest.

References

1. Bahrami, M.; Abenojar, J.; Martínez, M.A. Comparative Characterization of Hot-Pressed Polyamide 11 and 12: Mechanical, Thermal and Durability Properties. *Polymers* **2021**, *13*, 3553, 1-21, https://doi.org/10.3390/polym13203553.

2. Wu, J.; Wang, Y.; Wang, Yi.; Guo, Y.; Hao, X.; Zhou, Q.; Gong, Y. Characterization, Antistatic Treatment and Spinnability of Bio-based Polyamide 5,6 Staple Fibers. *J. Macro. Sci. B.* **2021**, https://doi.org/10.1080/00222348.2021.2002996.
3. Sacchi, M.C.; Marcicano, J.P.P.; de Vasconcelos, F.B. Biodegradable Polyamide 6.6 for Textile Application . *J. Manag. Sustain.* **2021**, *11*, 100-110, https://doi.org/10.5539/jms.v11n2p100.
4. Sridhara, K.P.; Masso, F.; Olsén P.; Vilaseca, F., Strong Polyamide-6 Nanocomposites with Cellulose Nanofibers Mediated by Green Solvent Mixtures. *Nanomaterials* **2021**, *11*, 2127., 1-17, https://doi.org/10.3390/nano11082127.
5. Zhang, T.; Kang, H., Enhancement of the Processability and Properties of Nylon 6 by Blending with Polyketone. *Polymers* **2021**, *13*, 3403, 1-15, https://doi.org/10.3390/polym13193403.
6. El-Bakary, M. A. Determination of the Opto-Mechanical and Geometrical Properties of High Density Polyethylene Fibers. *Opt. & Laser Eng.* **2008**, *46*, 328-335, https://doi.org/10.1016/j.optlaseng.2007.11.007.
7. Lai, C.C.; Chen, S.Y.; Chen, M.H.; Chen, H.L.; Hsiao, H.T.; Liu, L.C.; Chen, C.M. Preparation and characterization of heterocyclic polyamide 6 (PA 6) with high transparencies and low hygroscopicities. *J. Mol. Str.* **2019**, *1175*, 836–843, https://doi.org/10.1016/j.molstruc.2018.08.032.
8. Shalaby, S.E.; Abo El-Ola, S.M.; Al-Balakocy, N.G.; Bilyakova, M.; Abas, R. Development of Pilot Scale System for Production of Polyamide-6 Fibers Grafted With Polymethacrylic Acid For Ion Exchange Applications *Egypt. J. Chem.* **2018**, *61*, 1097-1109, https://doi.org/10.21608/ejchem.2018.3631.1301.
9. Dawelbeit, A.; Yu, M. Tentative Confinement of Ionic Liquids in Nylon 6 Fibers: A Bridge between Structural Developments and High-Performance Properties. *ACS Omega* **2021,** *6* , 3535-3547, https://doi.org/10.1021/acsomega.0c04740.
10. Handwerker, M.; Wellnitz, J.; Marzbani, H.; Tetzlaff, U. Annealing of chopped and continuous fiber reinforced polyamide 6 produced by fused filament fabrication. *Compsites Part B* **2021**, *223*, 109119, https://doi.org/10.1016/j.compositesb.2021.109119.
11. Hamza, A.A.; Fouda, I.M.; Sokkar, T.Z.N.; El-Bakary, M. A. Opto- Thermal Properties of Fibers: 3-Effect of Anisotropic Optical Parameters in polypropylene Fibers as A function of Annealing Process. *Polym. Test.* **1996**, *15*, 245-268, https://doi.org/10.1016/0142-9418(95)00017-8.
12. Ali, A.M. The impact of the thermal annealing conditions on the structural properties of polylactic acid fibers. *Microsc. Res. Tech.* **2021**, 1-7, https://doi.org/10.1002/jemt.23956.
13. Boruvka, M.; Cermak, C.L.; Brdlik, P. Effect of In-Mold Annealing on the Properties of Asymmetric Poly(L-lactide)/Poly(D-lactide) Blends Incorporated with Nanohydroxyapatite . *Polymers* **2021**, *13*, 2835, https://doi.org/10.3390/polym13162835.
14. Sokkar, T.Z.N. ; El-Farahaty, K.A.; El-Bakary, M. A. Determination of Optical Properties, Dispersion and Some Structural Parameters of PET Fibers Using Automatic Variable Wavelength Interferometry Technique. J. Appl. Polym. Sci. **2003**, *89*, 1737-1742, https://doi.org/10.1002/app.12189.
15. Hamza, A.A.; Sokkar, T.Z.N.; El-Bakary, M. A.; Ali, A.M. An interferometric method for studying the influence of temperature on the mean refractive indices and cross-sectional area of irregular fibers. Polym. Test. **2003**, *22*, 83-91, https://doi.org/10.1016/S0142-9418(02)00053-3.
16. Sokkar, T.Z.N.; El-Bakary, M.A.; Raslan, M.I.; Sewidan, M.A.; Hamza, A.A. A hybrid method of phase shifting interferometry and optical tomographic techniques for determining the optical anisotropy of grafted nylon-6 fibers with PMMA polymer. *Optik* **2022**, *251*, 168485, https://doi.org/10.1016/j.ijleo.2021.168485.
17. Roiron, C.; Lainé, E.; Grandidier, J.; Garois, N.; Vix-Guterl , C. A Review of the Mechanical and Physical Properties of Polyethylene Fibers. *Textiles* **2021**, *1*, 86–151, https://doi.org/10.3390/textiles1010006.
18. Barakat, N.; Hamza, A.A. Interferometry of fibrous materials. *Adam Hilger, Bristol* **1990**, https://www.taylorfrancis.com/books/mono/10.1201/9781003069492/interferometry-fibrous-materials-barakat-hamza.
19. Pluta, M. Advanced light Microscopy. *Vol. 3 PWN Warrsaw, Poland* **1993**. ISBN-13: 978-0-444-98819-5.
20. Sokkar, T.Z.N.; El-Bakary, M.A. Determintion of the refractive index of fibers using the modified area method: I-Homogenous fibers., *Opt. & Laser Techno. 2004, 36,507-513*. https://doi.org/10.1016/j.optlastec.2004.01.001
21. El-Bakary, M. A. Determination of Refractive Index Profile of Partially and Highly Oriented Fibers Using Double Refracting Interference Microscopy., *J. Appl. Polym. Sci.* **2003**, *87*, 2341-2347, https://doi.org/10.1002/app.11915.

22. Sokkar, T.Z.N. ; El-Farahaty, K.A.; El-Bakary, M.A.; Omer, E.; Hamza, A.A. A modified method for accurate correlation between the craze density and the optomechanical properties of fibers using pluta microscope. *Micros. Res. Tech.* **2016**, *79*, 422-430, https://doi.org/10.1002/jemt.22645.
23. Sokkar, T.Z.N.; El-Farahaty, K.A.; El-Bakary, M.A.; Omer, E.; Hamza, A.A. Optical birefringence and molecular orientation of crazed fibers utilizing the phase shifting interferometric technique. *Opt. & Laser Techno.* **2017**, *94*, 208-216, https://doi.org/10.1016/j.optlastec.2017.03.037.
24. Hamza, A.A.; Sokkar, T.Z.N.; El-Bakary, M. A. Determining the optical properties of highly oriented fibers using a multiple-beam technique. *J. Opt A: Pure Appl. Opt.***2001**, *3*, 421-427, https://doi.org/10.1088/1464-4258/3/5/316.
25. Sokkar, T.Z.N.; El-Bakary, M.A. The Refractive Index Profile of Highly Oriented Fibers, *J. Phys. D: Appl. Phys.* **2001**, *34*, 373-378, https://doi.org/10.1088/0022-3727/34/3/321.
26. El-Bakary, M. A. Determination of radial structural properties and spectral dispersion curves of poly(aryl ether ether ketone) fiber. *Polym. Inter.***2004**, *53*, 48- 55, https:///doi.org/10.1002/pi.1201.
27. Sokkar, T.Z.N.; El-Bakary, M.A.; Sewidan, M.A.; Hamza, A.A. FECO fringes for investigating the dispersion and mechanical properties of polyamaide-6 fibers grafted with PMMA" *Micro. Res. Tech.* **2021**, *84*, 3104–3115, https://doi.org/10.1002/jemt.23868.
28. Wypych, G. Handbook of polymers (*3rd ed. chap.68, ChemTec Publishing Elsevier* **2016**, https://www.elsevier.com/books/handbook-of-polymers/wypych/978-1-927885-95-6.
29. Microinterferometer Operation User Manual by Institute of Applied Optics Staff members, Automatic Computer-Aided Microinterferometer for Measurements and Studies of Optical and Textile Fibers. (*Institute of Applied Optics, Warsaw, Poland*.
30. Wemple, S.H. Material dispersion in optical fibers. *Appl Opt.* **1979**, *18*, 31–35, https://www.osapublishing.org/ao/abstract.cfm?URI=ao-18-1-31.
31. Badran, H. A. Study on Optical Constants and Refractive Index Dispersion of Neutral red Doped Polymer Film. *A.J. Appl. Sci.* **2012**, *9*, 250-253, https://doi.org/10.3844/ajassp.2012.250.253.
32. Lee, P.A.; Said, G.; Davis, R.; Lim, T.H. On the optical properties of some layer compounds. *J Phys Chem Solids* **1969**, *30*, 2719–2729, https://doi.org/10.1016/0022-3697(69)90045-6.
33. Samuels, J. R. Structure Polymer Properties, *John Wiley* **1975**, *54*, https://doi.org/10.1016/00323861(75)90265-7.
34. Kołbuk, D.; Sajkiewicz P.; Kowalewski, T. A. Optical birefringence and molecular orientation of electrospun polycaprolactone fibers by polarizing-interference microscopy. *Eur. Polym. J.* **2012**, *48*, 275-283, https://doi.org/10.1016/j.eurpolymj.2011.11.012.
35. De Vries, H.; Bonnebat, C.; Beautemps, J. Uni- and biaxial orientation of polymer films and sheets. *J. Polym. Sci. Symp.* **1977**, *58*, 109–156, https://doi.org/10.1002/polc.5070580111.
36. Zhao, P.; Peng, Y.; Yang, W.; Fu, J.; Turng, L.S.; Zhao, P.; Peng, Y.; Yang, W.; Fu, J.; Turng Vasanthan, L.S. Orientation and Structure Development in Polyamide 6 Fibers upon Drawing. *J. Polym. Sci. Part B: Polym. Phys.* **2003**, *41*, 2870 –2877, https://doi.org/10.1002/polb.10605.
37. Angad, H.; Gaur, H.; De Vries, H. On the refractive indexes and birefringence of nylon 6 yarns as a function of draw ratio and strain. *J. Polym. Sci. Phys. Ed.* **1975**, *13*, 835-850, https://doi.org/10.1002/pol.1975.180130415.
38. Zhao, P.; Peng, Y.; Yang, W.; Fu, J.; Turng, L. Crystallization measurements via ultrasonic velocity: study of poly (lactic acid) parts *J. Polym. Sci. B: Polym. Phys.* **2015**, *53*, 700-708, https://doi.org/10.1002/polb.23691.